Role of an N-Terminal Site of Ubc9 in SUMO-1, -2, and -3 Binding and Conjugation[†]

Michael H. Tatham,[‡] Suhkmann Kim,[§,‖] Bin Yu,[§] Ellis Jaffray,[‡] Jing Song,[§,⊥] Jian Zheng,[§] Manuel S. Rodriguez,[#] Ronald T. Hay,[‡] and Yuan Chen*,[§]

Division of Immunology and Graduate School of Biological Sciences, Beckman Research Institute of the City of Hope, 1450 East Duarte Road, Duarte, California 91010, Center for Biomolecular Sciences, University of St. Andrews, St. Andrews, Scotland, and Institut Jaques Monod, Tour 43-44, 2, place Jussieu 75005, Paris, France

Received April 2, 2003; Revised Manuscript Received June 16, 2003

ABSTRACT: Covalent posttranslational modification of target proteins with ubiquitin and ubiquitin-like proteins regulates many important cellular processes. However, the molecular mechanisms by which these proteins are activated and conjugated to substrates has yet to be fully understood. NMR studies have shown that the ubiquitin-like proteins SUMO-1, -2, and -3 interact with the same N-terminal region of the E2 conjugating enzyme Ubc9 with similar affinities. This is correlated to their almost identical utilization by Ubc9 in the SUMO conjugation pathway. To investigate the functional significance of this interaction, site-directed mutagenesis was used to alter residues in the SUMO binding surface of Ubc9, and the effect of the amino acid substitutions on binding and conjugation to SUMO-1 and target protein RanGAP1 was investigated by isothermal titration calorimetry and biochemical analysis. R13A/K14A and R17A/K18A mutations in Ubc9 disrupted the interaction with SUMO-1 but did not completely abolish the interaction with E1. While these Ubc9 mutants displayed a significantly reduced efficiency in the transfer of SUMO-1 from E1 to E2, their ability to recognize substrate and transfer SUMO-1 from E2 to the target protein was unaffected. These results suggest that the noncovalent binding site of SUMO-1 on Ubc9, although distant from the active site, is important for the transfer of SUMO-1 from the E1 to the E2. The conservation of E2 enzymes across the ubiquitin and ubiquitin-like protein pathways indicates that analogous N-terminal sites of E2 enzymes are likely to have similar roles in general.

Covalent attachment of ubiquitin and ubiquitin-like proteins (Ublps) to protein targets are important posttranslational modifications that regulate many significant cellular processes (*1*, *2*). The SUMO[1] family of Ublps has recently been shown to play important roles in various cellular functions (*3*−*5*). Three SUMO paralogues have been reported in mamalian cells, known as SUMO-1, -2, and -3 (*6*, *7*), although the bulk of the current research has concentrated on SUMO-1. In contrast to ubiquitination, which in most cases targets proteins for proteasome-mediated degradation, SUMO-1 modification of target proteins is known to result

in a number of substrate specific functions. SUMO-1 modification of RanGAP1 is required for its localization to the nuclear pore complex (NPC) (*8*, *9*), while SUMO-1 modification of PML is required for the correct assembly of nuclear bodies (*10*, *11*). Modification of the transcriptional inhibitor IκBα by SUMO-1 takes place at the same Lys residue (Lys21) as ubiquitin conjugation and thus inhibits ubiquitination and stabilizes IκBα (*12*). SUMO-1 modification has also been shown to result in activation of the transcription factor p53 and a heat shock transcription factor (*13*−*15*) and conversely bring about transcriptional repression when LEF and myb are modified (*16*, *17*).

SUMO-2 and -3 are closely related and share 97% amino acid sequence identity. However, these two proteins are only 46−48% identical to SUMO-1 and unlike SUMO-1 have the ability to form polymeric chains (*18*). The targets and the in vivo functions of SUMO-2 and -3 modifications are still not well-understood but appear to be distinct from that of SUMO-1 (*19*).

Different Ublps are conjugated to protein targets by specific, three-step modification pathways. Each Ublp is first activated by a distinct E1 enzyme (*1*−*3*), which forms a high-energy thiolester bond between the -SH group of its active site Cys and the C-terminal -COOH group of the Ublp in an ATP-dependent process. The Ublp is then transferred to the cognate conjugation enzyme (E2) by forming a thiolester bond with the -SH group of the active site Cys residue of

* To whom correspondence should be addressed. Tel: (626) 930-5408. Fax: (626) 301-8186. E-mail: ychen@coh.org.

[‡] University of St. Andrews.

[§] Division of Immunology, Beckman Research Institute of the City of Hope.

[‖] Current Address: Department of Physics, Pusan National University, Pusan 609-735, Korea.

[⊥] Graduate School of Biological Sciences, Beckman Research Institute of the City of Hope.

[#] Institut Jaques Monod.

[1] Abbreviations: SUMO, small ubiquitin-like modifier; E2, SUMO or ubiquitin conjugating enzyme; Ubc9, E2 for the SUMO-1 pathway; E1, SUMO or ubiquitin activating enzyme; SAE1/SAE2, the heterodimer composed of SAE1 and SAE2 subunits that function as the E1 enzyme for the SUMO pathway; ITC, isothermal titration calorimetry; E3, ubiquitin ligases; NMR, nuclear magnetic resonance spectroscopy; 1-D, one-dimensional.

the E2. In the final step, the Ublp is attached to target proteins by the formation of an isopeptide bond between its C-terminal -COOH group and the ϵ-amino group of a specific Lys residue on the target protein. In the SUMO-1 pathway, the Lys is usually found within a conjugation consensus motif ψKxE (where ψ represents a hydrophobic residue, K the target lysine, and E a glutamic acid) (*20*). Recently, a number of proteins with E3-like activity in the SUMO pathway have been identified, which are thought to increase the rate of the SUMO conjugation reaction (*17, 21−24*).

The molecular mechanisms of modifications by Ublps are being investigated by both X-ray and NMR studies. A noncovalent complex between SUMO-1 and Ubc9 has been identified and analyzed by NMR spectroscopy showing that SUMO-1 binds specifically to a surface near the N-terminus in Ubc9 that is distant from the active site Cys (*25*). A similar noncovalent interaction has also been identified between the equivalent surfaces on ubiquitin and the ubiquitin conjugating enzyme Ubc2b (*26*), showing that this association between E2 and modifier is not unique to Ubc9 and SUMO.

To investigate the significance of the noncovalent interaction between Ubc9 and SUMO, we have compared the binding of SUMO-1, -2, and -3 to Ubc9 by NMR chemical shift perturbation. The results show that despite significant sequence differences between the SUMO proteins, they bind to the same N-terminal region of Ubc9 with similar affinity. In addition, conjugation activities of the three SUMO proteins to E1 and Ubc9 were also compared to determine whether their in vivo differences in conjugation to target proteins are related to the E1 and E2 enzymes. To investigate the role of the SUMO-Ubc9 interaction, mutant forms of Ubc9 were generated in which the residues at the binding surface for the SUMO proteins have been altered. As expected, the mutants disrupted the noncovalent interaction between SUMO-1 and Ubc9. Although the amino acid substitutions are more than 30 Å away from the active site Cys93, SUMO-1·Ubc9 thiolester bond formation and the overall conjugation activity were both dramatically reduced, without significantly altering substrate recognition or affecting the transfer of SUMO-1 from Ubc9 to a target protein. These data indicate that the N-terminal region of Ubc9 contains an identical binding site for all three SUMO proteins, and this region plays an important role in the SUMO-1 conjugation pathway.

MATERIALS AND METHODS

cDNA Cloning. The R13A/K14A and R17A/K18A-Ubc9 mutants were created using a three-stage PCR process as described previously (*27*) using the external primers 5′-CCAAGCGGGAGCCCAAGCTTGTCGACATGCTTATGA-GGGCGCAAACTTCTTGG-3′ and 5′-GAAGGAGATATA-CCATGGGCCATCATCATC-3′; the D-primer: 5′-CCAAGC-GGAGCCC-3′; and the mutant internal primers: 5′-CTCGC-CCAGGAGAGGAAAGCATGGGCGGCA-3′ (R13A/K14A) and 5′-AGCAGACTCGCCCAGGAGGCGGCAGCAGCAT-GG-3′ (R17A/K18A). Wild-type (wt) human Ubc9 and the mutants were subcloned into vector PET28 as described previously (*25*). The modified plasmids have an open reading frame that encodes the His$_6$-tag at the N-terminus of the Ubc9 constructs.

The human RanGAP1$_{418−587}$ construct was generated by single-stage PCR using the primers 5′-CGCGGATCCAA-

CACTGGGGAGCCAGCT-3′ and 5′-CCGGAATTCCTA-GACCTTGTACAGCGT-3′ and wt-RanGAP1 DNA as a template. PCR products were cleaved with *Bam*HI and *Eco*RI restriction enzymes and ligated into similarly digested pGEX-2T plasmid for bacterial expression.

Protein Purification. Escherichia coli cells containing Ubc9 expression plasmids were grown and induced at 37 °C in LB media. Wild-type and mutant Ubc9 proteins were purified from cell lysates using nickel nitrilotriacetic acid columns under native conditions. Concentrations of the Ubc9 proteins were estimated by amino acid analysis at the Protein Core facility at the City of Hope.

GST-SUMO-1 (wt and C52A mutant), GST-SUMO-2 (wt and K11R mutant), GST-SUMO-3 (wt and K11R mutant), and the GST-fusion of residues 418−587 of RanGAP1 (GST-RanGAP1$_{418−587}$) proteins were expressed in *E. coli* strain B834 as described previously (*18*). GST-SUMO proteins were bound to glutathione−sepharose beads and cleaved by 17 U/mL thrombin while bound. The SUMO proteins were dialyzed against 20 mM ammonium bicarbonate pH 8.2, 1 mM DTT and then lyophilized before being dissolved in 50 mM Tris/HCl pH 7.5, 1 mM DTT to a concentration of 10 mg/mL. GST-RanGAP1$_{418−587}$ was purified by binding to glutathione−sepharose beads and eluted with 10 mM reduced glutathione. The GST moiety of GST-RanGAP1$_{418−587}$ was cleaved from a portion of the purified protein by thrombin, and after dialysis against 50 mM Tris/HCl pH 7.5, GST was removed by rebinding to glutathione−sepharose beads. The purity of all recombinant proteins was checked by SDS−polyacrylamide gel electrophoresis.

NMR Studies. The wt and mutant Ubc9 proteins were characterized by 1-D NMR experiments to ensure that the amino acid substitutions do not disrupt the overall structural integrity of the protein. The samples for NMR measurements, wt-Ubc9, R13A/K14A, and R17A/K18A mutants, were at 4, 2.7, and 4.2 mg/mL concentrations, respectively, in 95% H$_2$O/5% D$_2$O at pH 6.0. 1-D ^{1}H experiments were performed on a Varian Unity plus 500 spectrometer equipped with four channels, pulse shaping, and pulsed field gradient capabilities.

All NMR samples for the titration of SUMO-2 and -3 into Ubc9 contained 100 mM phosphate buffer (pH 6.0) in 95% H$_2$O/5% D$_2$O. The concentrations of protein samples were estimated with the Bio-Rad protein assay and a further ^{1}H 1-D NMR measurement. ^{1}H-^{15}N HSQC experiments (*28*) were performed with the digital resolutions of the spectra of 0.02 ppm in the proton dimension and 0.05 ppm in the amide ^{15}N dimension. For observing the SUMO-2/-3 binding site on Ubc9, 0.5 mM ^{15}N-labeled Ubc9 was used and titrated with unlabeled SUMO-2 and -3. The final concentrations of both proteins at the end of the titration were approximately 0.4 mM. The spectra were observed at 30 °C, a condition used for obtaining the resonance assignments of Ubc9. The NMR resonance assignments for Ubc9 have been described previously (*29*).

Measurement of Ubc9/SUMO-1 and Ubc9/RanGAP1$_{418−587}$ Binding Affinity using Isothermal Titration Calorimetry (ITC). The noncovalent associations between Ubc9 and the modifier SUMO-1 or the substrate RanGAP1$_{418−587}$ were measured by ITC using a VP-ITC microcalorimeter (Micro-Cal Inc., Northampton, MA) controlled by VPViewer 2000 software. All protein samples were buffered with 50 mM Tris/HCl pH 7.5/5 mM β-mercaptoethanol and were thor-

oughly degassed before use. ITC experiments were performed at 30 °C using 5 μcal/s reference power. The sample cell (1.4 mL) contained either 10 μM SUMO-1 or 10 μM RanGAP1$_{418-587}$, which were titrated against 200 μM Ubc9 (injectant) in 10 μL volumes. Experiments were either terminated after saturation or left to continue until all 20 programmed injections had occurred. Origin software (Micro-Cal v 5.0) was used to subtract blank runs (buffer titrated against Ubc9) for each Ubc9 protein, and where possible, to calculate binding constants. Experiments were either duplicated or triplicated to confirm constant calculations.

Detection of Ubc9-E1 Interaction by Gel Electrophoresis under Native Conditions. In a reaction volume of 13 μL, approximately 2 μg of human SAE1/SAE2 was incubated with approximately 8 μg of either the wild-type or the mutant Ubc9 protein samples in 50 mM Tris/HCl buffer at pH 7.5 with approximately 8% glycerol, 0.13 mM DTT for 20 min to 1 h at room temperature. The proteins were separated on a 5% native polyacrylamide gel and detected by silver staining.

SUMO-1 Transfer Assays from Ubc9 to GST-Ran-GAP1$_{418-587}$. To examine the effect of the N-terminal mutations of Ubc9 on the second step of Ubc9 reaction (target protein binding and isopeptide bond formation), preformed ^{125}I-SUMO-1·Ubc9 thiolester complexes were added to recombinant GST-RanGAP1$_{418-587}$ protein in 10 μL in vitro reactions, and the formation of ^{125}I-SUMO-1-substrate conjugates was measured over time. ^{125}I-SUMO-1·Ubc9 thiolesters were formed in 3.3 mM ATP, 8.3 mM MgCl$_2$, 67 mM Tris/HCl pH 7.5, and 67 U·mL^{-1} IPP in the presence of 0.24 μM SAE1/SAE2, 6 μM ^{125}I-C52A-SUMO-1, and 1 μM wt-Ubc9 or 10 μM R13A/K14A or R17A/K18A-Ubc9. Higher concentrations of the mutants were required to allow accumulation of approximately equal quantities of Ubc9·SUMO-1 thiolester complexes because of the mutations negatively affecting this reaction. Reactions were incubated between 3 and 30 min at 37 °C to accumulate between 0.4 and 0.6 μM Ubc9·SUMO-1 complexes. ATP-dependent reactions was halted by addition of 20 mM EDTA, which inhibits any further ATP-dependent thiolester formation. At this point, Ubc9 was added to the wt reaction mixture to bring the concentration to the same level as that of the mutants (10 μM). This eliminates any differences between samples that may have occurred because of differing concentrations of uncomplexed Ubc9. Because of the velocity of the transfer reaction, all solutions and equipment were then cooled to 4 °C. A sample of each reaction was taken prior to transfer initiation representing the zero time-points. Transfer reactions were then started by addition of GST-RanGAP1$_{418-587}$ to a final concentration of 0.2 μM. Samples were taken after 10, 20, 30, and 60 s and halted by addition to 4 M urea/SDS sample buffer lacking reducing agent. Reaction products were fractionated on 8−10% polyacrylamide gels containing SDS, which were stained and destained before drying and analysis by phosphorimaging. Quantitative analysis of phosphorimage results allowed the calculation of the concentration of the newly formed RanGAP1$_{418-587}$−SUMO-1 for each time-point and hence the % substrate converted to product. Recombinant C52A-SUMO-1 was radiolabeled with ^{125}iodine using the chloramine-T method as described previously (*18*). The mutant form was used instead of the wild-type protein to avoid experi-

mental complications from SUMO-1·SUMO-1 disulfide linked dimers. The GST-fusion form of Ran-GAP1$_{418-587}$ was used to produce a conjugated product of distinct molecular weight.

SUMO-1 Thiolester Transfer Assays from SAE1/SAE2 to Ubc9. To determine the effect of the Ubc9 mutants on the E1 to E2 SUMO-1 transfer step, an assay that monitors the rate of the transesterification reaction of ^{125}I-labeled SUMO-1 from SAE1/SAE2 to Ubc9 was employed. First, a ∼0.25 μM SAE1/SAE2·SUMO-1 thiolester complex was formed by the incubation at 37 °C for 60 min of a reaction containing 6.9 mM ATP, 0.14 U mL^{-1} IPP, 17.4 mM MgCl$_2$, 138.9 mM Tris/HCl pH 7.5, 0.51 μM SAE2/SAE1, and 2.46 μM ^{125}I-SUMO-1. To halt the reaction, EDTA was added to 30 mM. As described above, samples were taken after EDTA addition to represent zero time-points. All assay solutions and equipment were then cooled to 4 °C before addition of Ubc9. Time-course reactions were started by addition of the SAE2·SUMO-1 mix to solutions of varying Ubc9 concentration. In these assays, the final concentration of SAE2·SUMO-1 was ∼0.12 μM and Ubc9 was 5, 2, 1, 0.5, or 0.2 μM. Ten μL samples were removed and terminated after 10, 20, 30, and 60 s as described above. Reaction products were fractionated on polyacrylamide gels containing SDS, and gels were processed as described above. Radioactive species were detected and quantitated by phosphorimaging allowing the calculation of the % SUMO-1 transferred from SAE1/SAE2 onto each Ubc9 protein at each concentration.

^{125}I-SUMO Competition Assays. SAE1/SAE2·SUMO thiolester complex formation competition assays were performed in 10 μL reaction volumes containing 2.5 mM ATP, 5 mM MgCl$_2$, 50 U·mL^{-1} IPP, 50 mM Tris pH 7.5, 0.36 μM SAE1/SAE2, and 3.5 μM ^{125}I-C52A-SUMO-1 with either no competitor or with one of 10 1:1 serial dilutions of wt-SUMO-1, K11R-SUMO-2, and K11R-SUMO-3 (from 72.0 to 0.14 μM). Ubc9·SUMO thiolester formation assays were prepared in the same way but in the presence of 0.41 μM Ubc9 and using a range of competing SUMO from 80 to 0.15 μM. Under these conditions, the rate of formation of SAE1/SAE2·SUMO-1 or Ubc9·SUMO thiolester complexes was known to be proportional to SAE1/SAE2 or Ubc9 concentration, respectively. Reactions were incubated for 10 min at 37 °C before termination with SDS sample buffer, followed by electrophoresis in a 10% polyacrylamide gel containing SDS. Gels were stained and destained before drying and the phosphorimaging analysis. The mutant SUMO constructs C52A-SUMO-1 and K11R-SUMO-2/-3 were used to avoid experimental interference from SUMO-1−SUMO-1 disulfide linked dimers and the formation of poly SUMO-2 and SUMO-3 chains.

RESULTS

SUMO Paralogues Have a Conserved Surface for Binding Ubc9. SUMO-2 and 3 appear to have in vivo functions that differ from SUMO-1, as their conjugation to target proteins appears to be stimulated by environmental stresses, which do not appear to trigger SUMO-1 conjugation (*19*). As shown previously (*25*), the Ubc9 binding site on SUMO-1 mainly involves the β-sheet, including residues 27−32, 38, 63−71, and 82−90. Despite the fact that SUMO-2 and -3 share only ∼50% sequence identity with SUMO-1, the level of con-
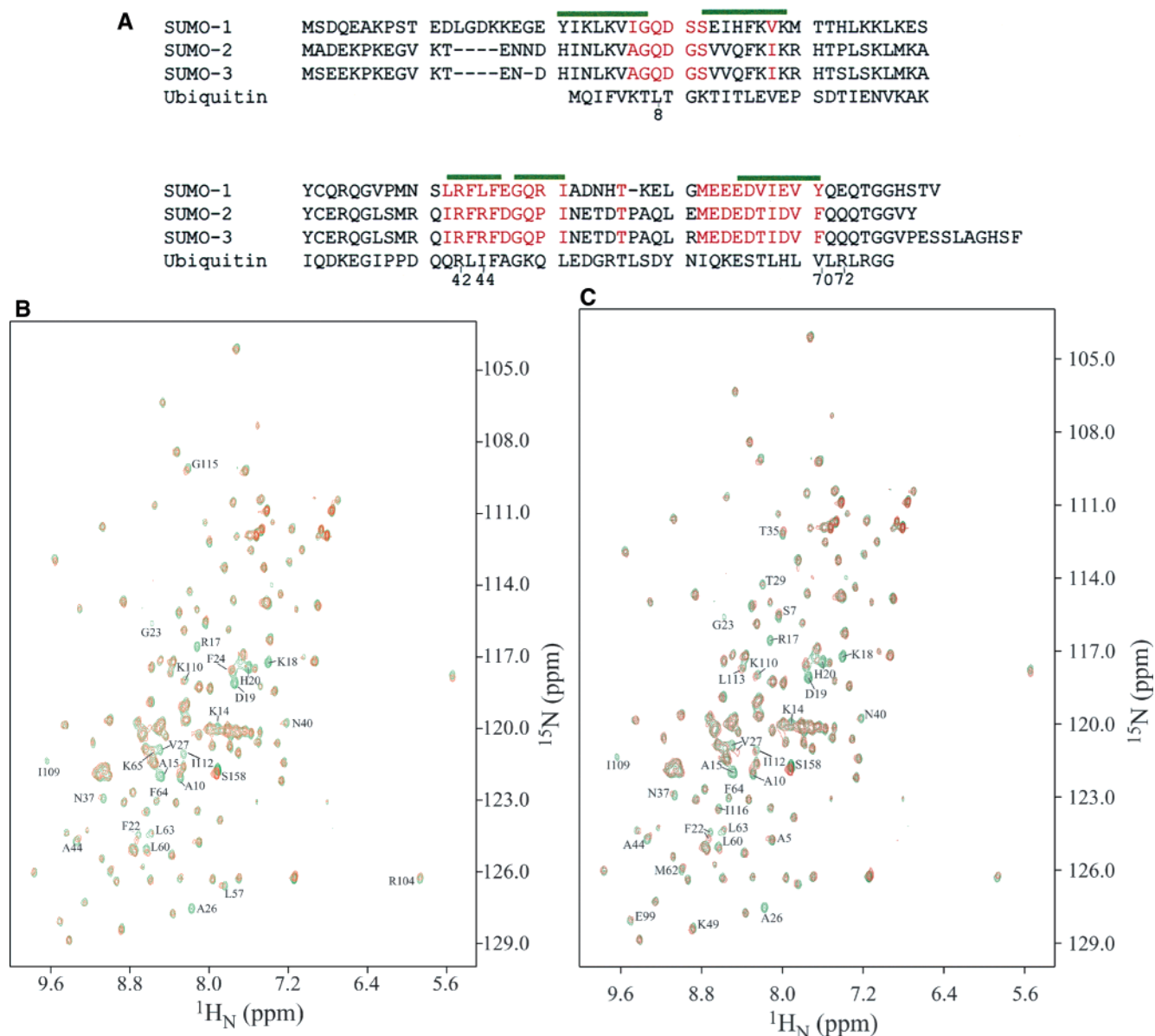
A

```
SUMO-1    MSDQEAKPST EDLGDKKEGE YIKLKVIGQD SSEIHFKVKM TTHLKKLKES
SUMO-2    MADEKPKEGV KT----ENND HINLKVAGQD GSVVQFKIKR HTPLSKLMKA
SUMO-3    MSEEKPKEGV KT----EN-D HINLKVAGQD GSVVQFKIKR HTSLSKLMKA
Ubiquitin                      MQIFVKTLT GKTITLEVEP SDTIENVKAK
                                       8
```

```
SUMO-1    YCQRQGVPMN SLRFLFEGQR IADNHT-KEL GMEEEDVIEV YQEQTGGHSTV
SUMO-2    YCERQGLSMR QIRFRFDGQP INETDTPAQL EMEDEDTIDV FQQQTGGVY
SUMO-3    YCERQGLSMR QIRFRFDGQP INETDTPAQL RMEDEDTIDV FQQQTGGVPESSLAGHSF
Ubiquitin IQDKEGIPPD QQRLIFAGKQ LEDGRTLSDY NIQKESTLHL VLRLRGG
                            42 44                        70 72
```

B

C

FIGURE 1: (A) Sequence alignment of SUMO-1, -2, -3, and ubiquitin. The amino acid residues in SUMO-1 that were shown to have significant chemical shift perturbation upon binding Ubc9 are indicated in red. Residues in SUMO-2 and -3 that are homologous to those indicated in red in the sequence of SUMO-1 are also shown in red. (B and C) ^{1}H-^{15}N HSQC spectra of ^{15}N-labeled Ubc9 in complex with unlabeled (B) SUMO-2 and (C) SUMO-3. The concentrations of Ubc9 and SUMO-2 or -3 were 0.4 mM. The spectra were acquired at 30 °C.

servation in the Ubc9 binding surface is very high between the three proteins (Figure 1A), suggesting that they bind to Ubc9 in a manner similar to SUMO-1.

To confirm that the binding of SUMO-2 and -3 to Ubc9 is similar to that of SUMO-1 to Ubc9, we used NMR chemical shift perturbation to probe the interactions. The binding surfaces of SUMO-2 and -3 on Ubc9 were investigated using ^{15}N-labeled Ubc9 in complexes with unlabeled SUMO-2 or -3. ^{1}H-^{15}N HSQC spectra of Ubc9, free and in complex with SUMO-2 or -3, were compared and analyzed. Both SUMO-2 and -3 produced very similar chemical shift perturbation and nearly identical changes in line widths as SUMO-1 in the ^{1}H-^{15}N HSQC spectrum of Ubc9 upon complex formation with Ubc9. Superposition of the HSQC spectra of SUMO-2 in 1:1 complex with Ubc9 and free Ubc9 is given in Figure 1B and that of SUMO-3 is given in Figure 1C.

Specifically, upon complex formation with SUMO-2, the line widths of residues Ala[15], Arg[17], Lys[18], Asp[19], Gly[23], Ala[26], and Val[27] in Ubc9 became so broad in the complex that their cross-peaks cannot be observed. Residues Ala[10], His[20], Phe[22], Phe[24], Asn[37], Ala[44], Leu[57], Leu[60], Lys[65], Ile[109], Ile[112], Ser[158], and Gly[115] showed significant chemical shift perturbations. A few residues on this surface, including Leu[9], Asn[11], Glu[12], Arg[13], Gln[111], and Leu[114], have resonances that overlap with other resonances and therefore could not be monitored. The region of Ubc9 that interacts with SUMO-2, as suggested by the chemical shift perturbations, is identical to that of SUMO-1 as described previously.

The chemical shift changes and line-broadening effect observed in Ubc9 upon the complex formation with SUMO-3 are similar to those observed upon complex formation with SUMO-1 and -2. Some Ubc9 residues including Ala[15], Arg[17], Lys[18], Asp[19], Gly[23], and Ala[26] show a dramatic line-

broadening effect in the complex, and their cross-peaks disappeared gradually by titration of SUMO-3. Residues Ser[7], Ala[10], Lys[14], His[20], Phe[22], Val[27], Thr[35], Asn[37], Ala[44], Lys[49], Leu[60], Met[62], Leu[63], Glu[99], Ile[109], Lys[110], Ile[112], Leu[113], and Ser[158] show significant chemical shift changes upon titration with SUMO-3. Other residues that had larger increases in line widths than average but had small chemical shift changes are also labeled in the spectra in Figure 1C. These residues are found close to the region that showed the largest perturbation upon the formation of the complex. The most significant chemical shift perturbation upon SUMO-3 binding occurs in the same region of Ubc9 that interacts with SUMO-1 and -2.

Binding of both SUMO-2 and -3 to Ubc9 resulted in similar line-broadening effects to what was observed in the binding studies of SUMO-1 on Ubc9 (*25*). Similar line-broadening effects suggest that the affinities of the complex formation between Ubc9 and the three SUMO molecules are similar.

SUMO-1, -2, and -3 Form SUMO·SAE2/SAE1 and SUMO· Ubc9 Thiolester Complexes with Almost Equal Efficiency. To test whether SAE1/SAE2 and Ubc9 descriminate between the three SUMO proteins, competition analysis was carried out to compare the ability of SUMO-1, -2, and -3 to form thiolester complexes with SAE1/SAE2 and Ubc9. In this experiment, ^{125}I-labeled C52A-SUMO-1 was incubated with a range of concentrations of unlabeled SUMO-1, -2, and -3 in the presence of SAE1/SAE2 alone or together with Ubc9. For each analysis, the concentrations of SAE1/SAE2 and Ubc9 were both in the ranges that were shown to be rate-limiting for complex formation (data not shown). After incubation, the reaction products were separated by SDS—polyacrylamide gel electrophoresis, and the ^{125}I-SUMO-1· SAE2/SAE1 or Ubc9 thioester complexes were quantitated by phosphorimaging. Addition of increasing amounts of unlabeled SUMO-1, -2, and -3 to the reaction results in a dose-dependent decrease in the amount of ^{125}I-SUMO-1 conjugated to SAE1/SAE2 (Figure 2A) and Ubc9 (Figure 2B). Each form of SUMO competes with almost equal efficiency for the formation of ^{125}I-SUMO-1·SAE2 and ^{125}I-SUMO-1·Ubc9. This indicates that under these conditions SAE1/SAE2 and Ubc9 do not significantly discriminate between the various forms of SUMO, which is consistent with the observation that Ubc9 binds to SUMO-1, -2, and -3 using an identical binding surface and with similar affinity.

Mutations in Ubc9 that Alter the Interaction Surface with SUMO-1. The region of Ubc9 that interacts with the SUMO proteins in noncovalent complexes involves the surface consisting of part of the first α-helix, the first β-strand, and the loop between them as shown in Figure 3A (*25*). This surface has a strong positive electrostatic potential, and the amino acid residues in this region are highly conserved among Ubc9 orthologs as shown in Figure 3B. Residues Arg17 and Lys18 show the most significant chemical shift perturbation upon complex formation with SUMO, with residues Arg13 and Lys14 also displaying significant chemical shift changes. The locations of these positively charged residues in the 3-D structure of Ubc9 are indicated in Figure 3A. These four residues are in the N-terminal helix and were substituted with Ala in two Ubc9 double mutants, R13A/ K14A and R17A/K18A. Ala was chosen because it favors helical structures; thus, the substitutions are not likely to
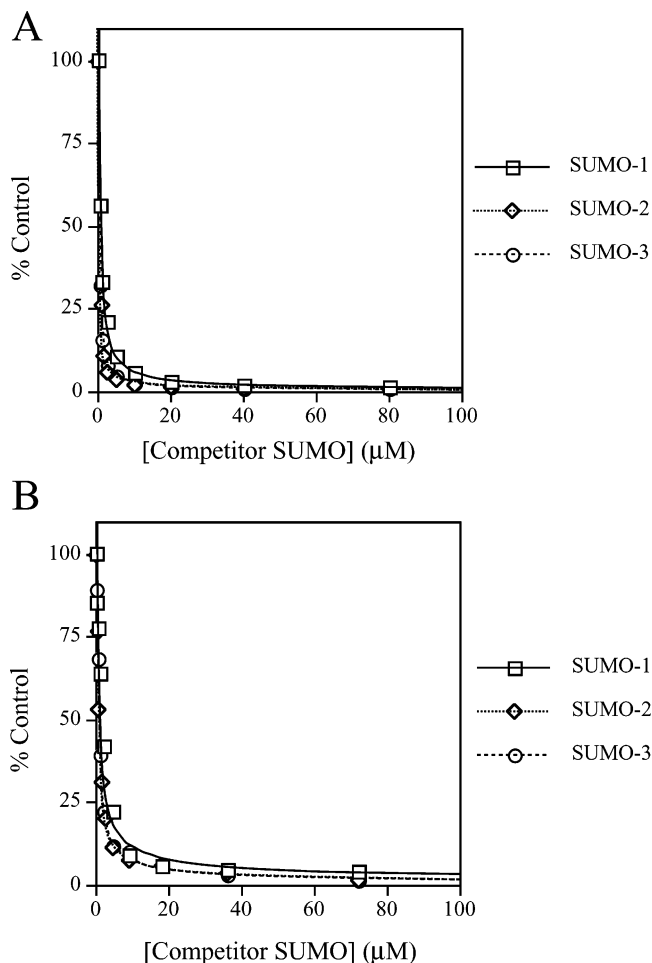

FIGURE 2: Competition for SAE1/SAE2 and Ubc9 thiolester complex formation by SUMO-1, -2, and -3. (A) Unlabeled SUMO-1, -2, and -3 competing with ^{125}I-labeled SUMO-1 for formation of thiolester complexes with SAE1/2. (B) Unlabeled SUMO-1, -2, and -3 competing with ^{125}I-labeled SUMO-1 for formation of thiolester complexes with Ubc9. Details of the experiment are given in the Materials and Methods.

disrupt the overall structure of Ubc9. Also, Ala substitution will reduce the positive electrostatic potential on this surface; thus, it is likely that these mutations will interfere with the protein—protein interaction.

The structural integrity of the mutant proteins was evaluated by 1-D NMR spectra. Figure 3C shows the 1-D spectra of the wild-type and mutant Ubc9 proteins. The region of the spectra displayed corresponds to signals of methyl and methylene groups, which include those from amino acid residues in the hydrophobic core of the protein, such as Ile, Leu, and Val. The 1-D spectra indicate that the amino acid substitutions do not disrupt the overall 3-D structure of the protein.

Effect of R13A/K14A and R17A/K18A Ubc9 Mutations on the Interactions with SUMO-1 and E1. To evaluate the effect of R13A/K14A and R17A/K18A-Ubc9 mutations, ITC was used to further investigate the noncovalent binding to SUMO-1. The binding of molecules to one another results in the release or absorbance of heat energy, and the heat changes can be measured with ITC to determine the binding constant, reaction stoichiometry, and a thermodynamic profile of the reaction. Wt-Ubc9 binds to SUMO-1 with a calculated stoichiometry of approximately 1:1 (Figure 4A). The non-
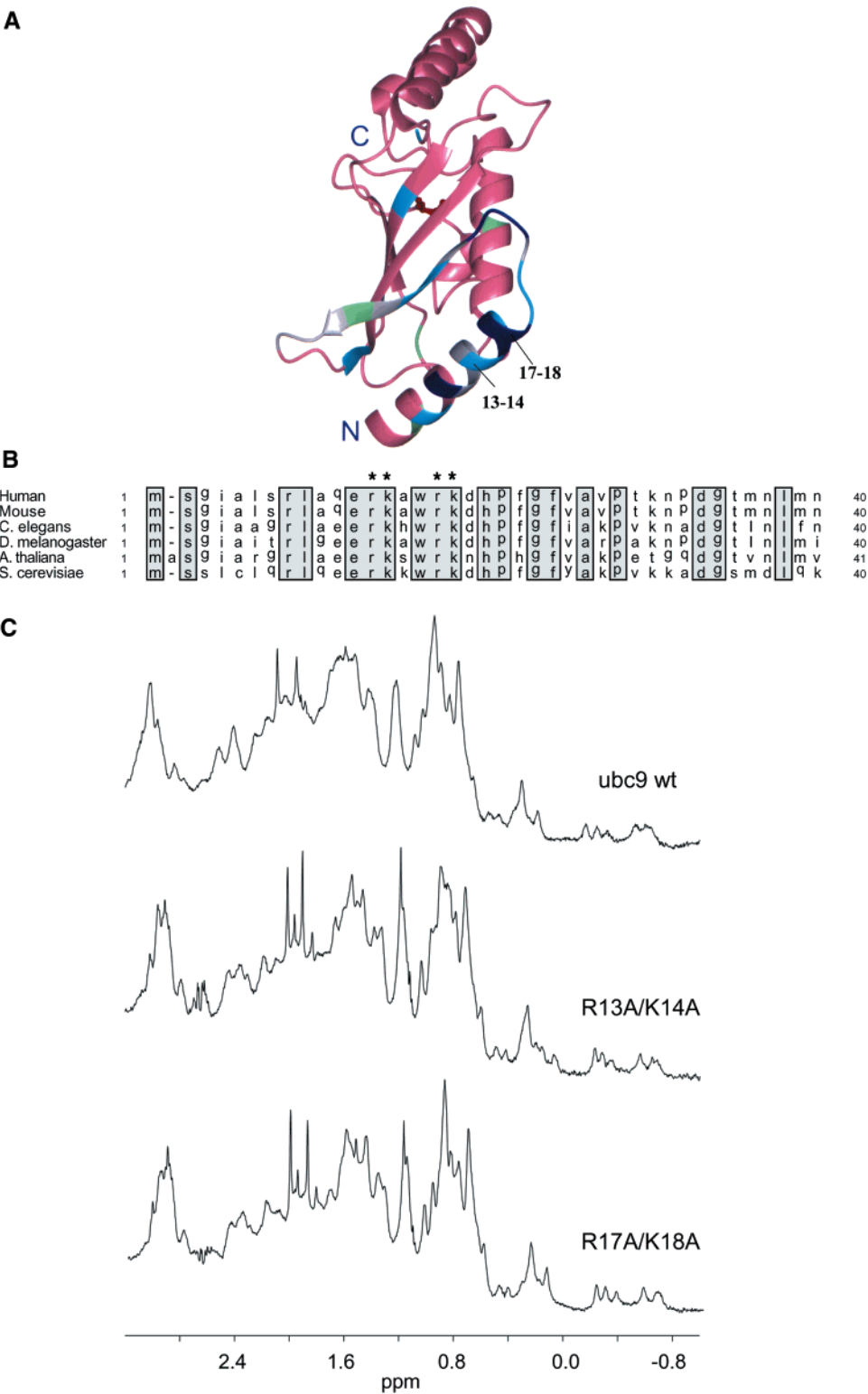
FIGURE 3: (A) Ribbon diagram of the 3-D structure of human Ubc9 showing the noncovalent SUMO-1 binding site. Residues that are not involved in binding SUMO-1 in the noncovalent complex are indicated in pink. The residues that show large, intermediate, or small but significant chemical shift perturbations upon forming a complex with SUMO-1 are indicated by dark blue, light blue, or green, respectively (*25*). The residues that cannot be monitored on this surface because of resonance overlap are shown in gray. The active site Cys[93] is shown with its side chain in red, and residues R13, K14, R17, and K18 are indicated in the structure. (B) Primary sequence alignment of the N-terminal region of Ubc9 homologues from different species. Identical residues are indicated by shaded boxes, and residues mutated in this study are highlighted by asterisks. (C) The amino acid substitutions of R13A/K14A and R17A/K18A do not disrupt the 3-D structures of Ubc9. 1-D NMR spectra of the two mutants R13A/K14A and R17A/K18A are shown along with the spectrum of wild-type Ubc9. The region of the 1-D spectra shown corresponds to the resonances of methyl and methylene groups, which include those located on residues in the hydrophobic core. Similarity between the three spectra indicates that the mutations did not disrupt the structural integrity of the protein.

covalent interaction between Ubc9 and SUMO-1 is strong with K_d being 0.25 μM $\pm$ 0.07 μM. The binding is both enthalpy driven with ΔH of -1990 ± 83.4 cal/mol and entropy driven with ΔS of 23.7 cal/mol/K. This is unusual
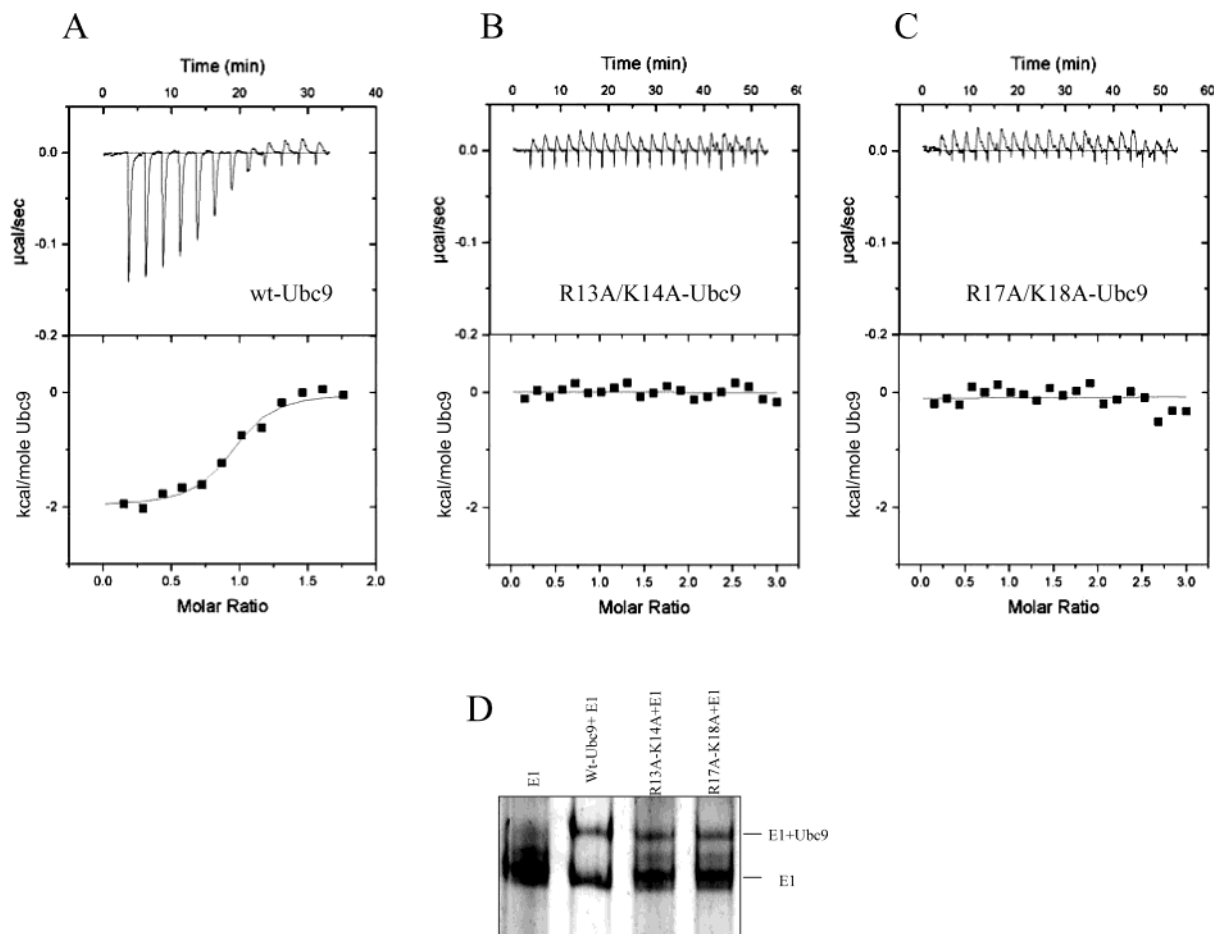
FIGURE 4: Isothermal calorimetric analysis of the noncovalent association between Ubc9 and SUMO-1. Raw (upper) and processed (lower) ITC analysis data for 1.4 mL of 10 μM SUMO-1 titrated with 10 μL injections of 200 μM wt-Ubc9 (A), R13A/K14A-Ubc9 (B), and R17A/K18A-Ubc9 (C). For wt-Ubc9, Origin software (MicroCal v 5.0) calculated the number of Ubc9 binding sites to be 0.91 ± 0.03, the binding enthalpy change (ΔH) to be −1990 ± 83.4 cal/mol, the entropy change (ΔS) to be 23.7 cal/mol/K, and the K_d to be 0.25 ± 0.07 μM. Deviation of the stoichiometry from one is likely due to uncertainties in concentration measurements of the two proteins. Because of the lack of measurable affinity for SUMO-1, binding parameters for the mutant Ubc9 proteins could not be calculated. (D) Gel electrophoresis to detect the Ubc9-E1 complex. Approximately 2 μg of human SAE1/SAE2 heterodimer was incubated with approximately 8 μg of either the wild-type or the mutant Ubc9 protein samples in 50 mM Tris HCl pH 7.5 with approximately 8% glycerol, 0.13 mM DTT for 20 min to 1 h at room temperature in a 13 μL volume. The proteins were separated on a 5% native polyacrylamide gel and detected by silver staining.

as complex formation is normally enthalpy driven with entropic penalties. The favorable entropic change is not likely due to conformational changes upon binding because chemical shift perturbation upon complex formation is localized to the binding surfaces (*25*). As both binding interfaces in Ubc9 and SUMO-1 contain hydrophobic residues, displacement of solvents from these surfaces upon complex formation is a more likely explanation for this observation, as found in other protein complexes (*30*, *31*).

The Ubc9 mutants, R13A/K14A and R17A/K18A, neither release nor absorb measurable heat upon titration into the solution containing SUMO-1, as shown in Figure 4B,C. The affinities of R13A/K14A and R17A/K18A-Ubc9 for SUMO-1 have been reduced to such an extent that the interaction cannot be detected by ITC measurement. Therefore, although the mutation did not disrupt the overall 3-D structure of Ubc9, it significantly reduced the noncovalent interactions with SUMO-1.

A recent study on the yeast SUMO-1 and Ubc9 orthologs Smt3p and Ubc9p has indicated that the E1 binding site partially overlaps with the SUMO-1 binding site on Ubc9 (*32*). In this study, the Ubc9-E1 interaction was examined

by gel electrophoresis under native conditions. We therefore employed a similar approach to determine the E1 binding ability of the Ubc9 mutants. R13A/K14A and R17A/K18A-Ubc9 both form complexes with E1, although their affinities for E1 are somewhat reduced as compared to that of the wild-type protein (Figure 4D). The fact that the protein−protein complexes can be observed in gel mobility shift assays indicates that the affinities of the Ubc9 mutants to E1 are still relatively high. Thus, this result suggests that residues 13, 14, 17, and 18 of Ubc9 may not be critical in forming interactions with E1 but are important for SUMO-1 binding.

R13A/K14A and R17A/K18A Ubc9 Proteins Are Defective in Overall Conjugation. To establish if the SUMO-1 binding site on Ubc9, which is distant from the active site, is important in the SUMO conjugation pathway, the R13A/K14A and R17A/K18A-Ubc9 mutants were tested in a SUMO conjugation assay using RanGAP1$_{418-587}$ as a substrate. The RanGAP1 fragment forms a stable complex with Ubc9 (*33*), which results in faster SUMO modification rates than other known SUMO substrates in the absence of an E3 enzyme. It is therefore unlikely that RanGAP1 requires an E3 enzyme for SUMO modification in vivo.
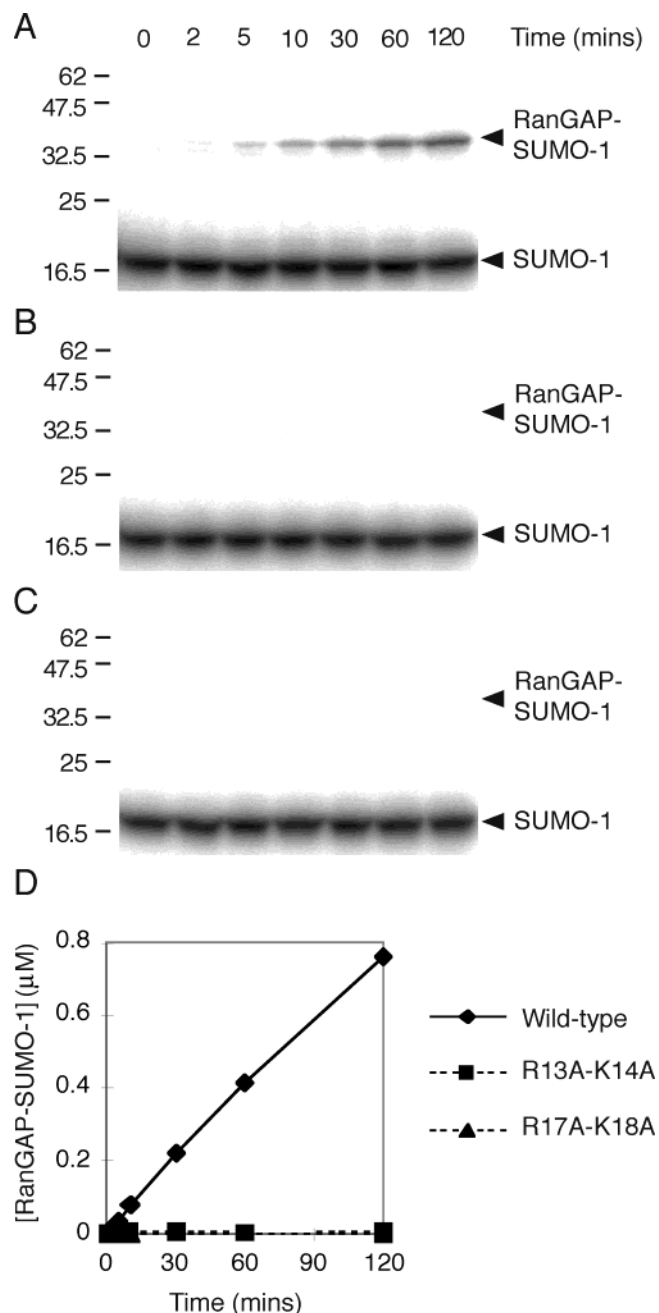
FIGURE 5: Effect of N-terminal Ubc9 mutations on the conjugation of SUMO-1 to the target protein RanGAP1$_{418-587}$. Reactions contained 0.56 μM Ubc9 (wild-type or mutants), 1.1 μM SAE1/SAE2, 5.24 μM ^{125}I-SUMO-1, 20 μM RanGAP1$_{418-587}$, and a buffered ATP regeneration system (50 mM Tris/HCl pH 7.5, 2 mM ATP, 10 mM creatine phosphate, 3.5 U mL^{-1} creatine kinase, 0.6 U mL^{-1} IPP, and 5 mM MgCl$_2$). Eighty μL batch assays were incubated at 37 °C, and 10 μL samples were removed at 0, 2, 5, 10, 30, 60, and 120 min (as indicated above panel A) before addition to protein sample buffer in the presence of reducing agent to halt the reaction. Samples were fractionated on 12% polyacrylamide gels containing SDS, which were stained, destained, and dried before phosphorimager analysis. The gels for the wt-Ubc9, R13A/K14A, and R17A/K18A-Ubc9 are shown in panels A−C, respectively. Molecular weight markers are indicated. Quantitation of the data is shown in panel D.

Conjugation of SUMO-1 to RanGAP1$_{418-587}$ proceeds efficiently in the presence of the wt-Ubc9 protein, increasing linearly with respect to time up to 120 min (Figure 5A,D). In contrast, neither R13A/K14A-Ubc9 (Figure 5B,D) nor R17A/K18A-Ubc9 (Figure 5C,D) is capable of catalyzing

the formation of significant amounts of RanGAP1$_{418-587}$−SUMO-1 conjugates after the reaction was carried out for 120 min (Figure 5B,C). Figure 5D is the quantitative representation of the data from gels in Figure 5A−C. These data suggest that the mutations of R13, K14, R17, and K18 of Ubc9 significantly reduce SUMO-1 conjugation activity in overall conjugation reactions.

R13A/K14A and R17A/K18A Mutants Do Not Alter Substrate Recognition by Ubc9. In the SUMO-1 conjugation pathway, Ubc9 is involved in two-step reactions, accepting SUMO-1 from E1 and transferring SUMO-1 to target proteins. These N-terminal mutations are not likely to affect substrate recognition by Ubc9 because the binding site of target proteins on Ubc9 has been identified recently as being centered around residue 129, which is close to the active site Cys93 in the 3-D structure of Ubc9 (*34, 35*). However, to confirm that the reduced overall conjugation activity by the N-terminal mutants were not due to altered substrate recognition by the Ubc9 protein itself, ITC analysis was employed to determine their binding affinities for RanGAP1$_{418-587}$. Upper panels of Figure 6 show the heat changes, which occur upon titration of the wild-type and mutant Ubc9 proteins into a solution of purified recombinant RanGAP1$_{418-587}$ in the ITC microcalorimeter. Figure 6A shows clearly that wt-Ubc9 binds strongly to RanGAP1$_{418-587}$ with a calculated K_d of 0.49 $\pm$ 0.02 μM and a binding stoichiometry of 1:1. The enthalpy change (ΔH) was calculated to be -12.1 ± 0.06 kcal/mol, and the entropy change (ΔS) was -10.9 cal/mol/K. The same experiment using the mutant R13A/K14A and R17A/K18A-Ubc9 gave very similar data (Figure 5B,C), as summarized in Figure 5D. Small differences in the ITC data between the wild-type and the mutant Ubc9 proteins could be due to uncertainties in concentration estimation of the proteins. The similar affinity of wt-Ubc9 and the mutants for RanGAP1$_{418-587}$ confirms that their reduced conjugation activity is not a consequence of poor substrate binding.

R13A/K14A and R17A/K18A Ubc9 Proteins Are Not Defective for the Transfer of SUMO-1 from Ubc9 to the Substrate. To further evaluate whether the R13A/K14A- and R17A/K18A-Ubc9 affect the transfer of SUMO-1 from Ubc9 to substrate proteins, experiments were performed to monitor the transfer of ^{125}I-labeled SUMO-1 from its thiolester complex with Ubc9 onto RanGAP1$_{418-587}$. Thiolester complexes of ^{125}I-SUMO-1 were formed with each of the Ubc9 proteins as described in the Materials and Methods. Approximately equal quantities of each wild-type and mutant Ubc9·SUMO-1 thiolester complex was formed before 20 mM EDTA was added to halt ATP-dependent thiolester formation, and a zero time sample was taken. The transfer reaction was initiated by addition of RanGAP1$_{418-587}$ substrate to 0.2 μM, and samples were taken at 10, 20, 30, and 60 s thereafter. Reactions were terminated by addition of 4 M urea/SDS sample buffer in the absence of reducing agent. Reaction products were fractionated by SDS/polyacrylamide gel electrophoresis and analyzed by phosphorimaging (Figure 7A). The relative quantities of ^{125}I-SUMO-1·Ubc9 complexes and ^{125}I-SUMO-1-RanGAP1$_{418-587}$ were determined and expressed graphically as % GST-RanGAP1$_{418-587}$ modified with respect to incubation time (Figure 7B). Inspection of the progress curves shows that the mutants have similar transfer rates as the wild-type protein and that the reduction
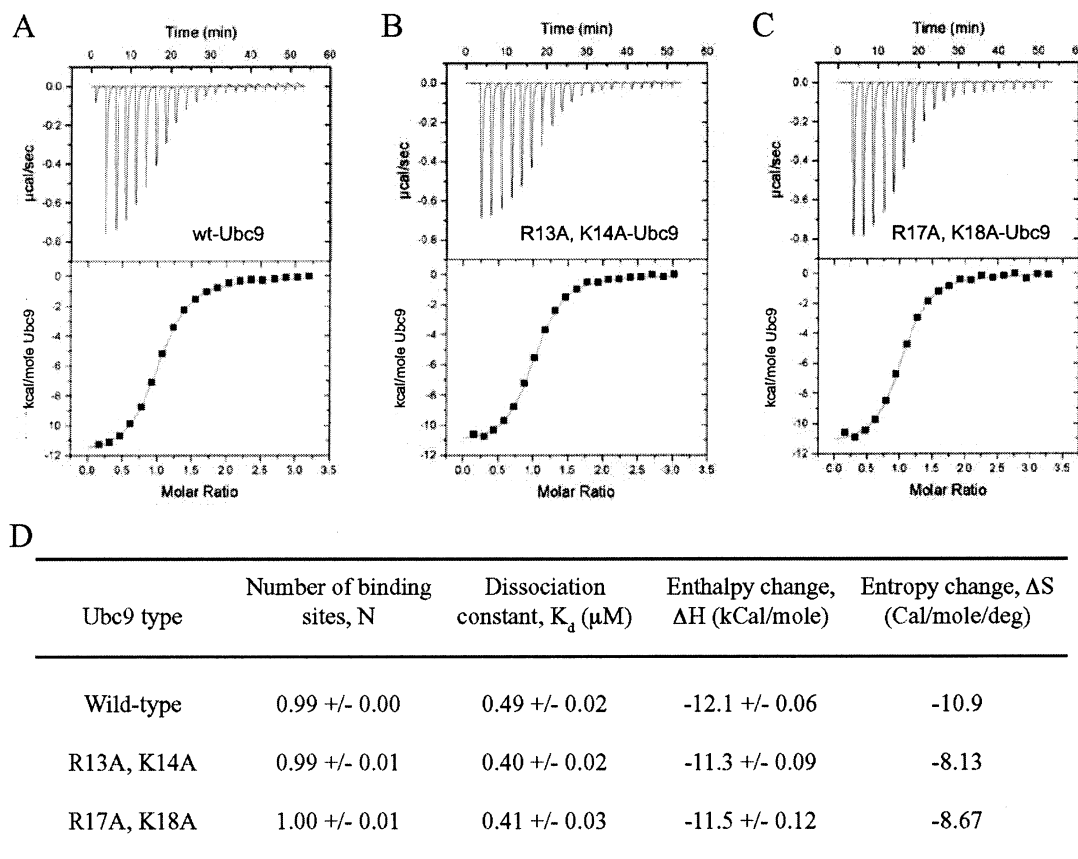
Ubc9 type	Number of binding sites, N	Dissociation constant, K_d (μM)	Enthalpy change, ΔH (kCal/mole)	Entropy change, ΔS (Cal/mole/deg)
Wild-type	0.99 +/- 0.00	0.49 +/- 0.02	-12.1 +/- 0.06	-10.9
R13A, K14A	0.99 +/- 0.01	0.40 +/- 0.02	-11.3 +/- 0.09	-8.13
R17A, K18A	1.00 +/- 0.01	0.41 +/- 0.03	-11.5 +/- 0.12	-8.67

FIGURE 6: Isothermal calorimetric analysis of the noncovalent association between Ubc9 and RanGAP1$_{418-587}$. Unprocessed (upper) and processed (lower) ITC analysis data for 1.4 mL of 10 μM RanGAP1$_{418-587}$ titrated with 10 μL injections of 200 μM wt-Ubc9 (A), R13A/K14A (B), and R17A/K18A-Ubc9 (C). As for wt-Ubc9 in Figure 2, Origin software (MicroCal v 5.0) was used to calculate the number of Ubc9 binding sites, the binding enthalpy change (ΔH), the entropy change (ΔS), and the K_d for each Ubc9 experiment. The results are tabulated in panel D. As ΔS is calculated directly from ΔH, the errors for each are directly proportional.

in the overall conjugation rates for the mutants is unlikely to involve this step of the conjugation pathway.

R13A/K14A and R17A/K18A Ubc9 Are Defective in Forming Thiolester Complexes with SUMO-1. In the SUMO-1 pathway, the first step of the reactions involving Ubc9 is the transfer of SUMO-1 from E1 to Ubc9. To establish if R13, K14, R17, and K18 of Ubc9 are important in forming the Ubc9·SUMO-1 conjugate, in vitro assays were carried out to monitor the rates of the transesterification reaction of ^{125}I-labeled SUMO-1 from SAE1/SAE2 to the mutant and wild-type Ubc9 proteins. In these experiments, the SAE1/SAE2·SUMO-1 thiolester complex was formed first, and then EDTA was added to halt the reaction. Time-course reactions were started by the addition of the SAE1/SAE2·SUMO-1 mix to solutions of varying Ubc9 concentration, and the transfer reactions were terminated after 10, 20, 30 and 60 s. Reaction products were fractionated under nonreducing conditions in polyacrylamide gels containing SDS. Figure 8A shows raw phosphorimage data of the transfer reactions for wt-Ubc9 (left), R13A/K14A-Ubc9 (center), and R17A/K18A-Ubc9 (right). The relative quantities of ^{125}I-SUMO-1·Ubc9 complexes and ^{125}I-SUMO-1·SAE2 were determined, as indicated above, and expressed graphically as % of SUMO-1 transferred with respect to incubation time. The results are represented graphically in Figure 8B−D for wild-type, R13A/K14A, and R17A/K18A-Ubc9, respectively. It is clear that both mutants have dramatically reduced activity relative to the wild-type protein in this step of the conjugation pathway. Since both mutants disrupted the

binding to SUMO-1, but were still able to form a complex with E1, it is likely that the dramatic effect of the mutants in the transfer of SUMO-1 from E1 to E2 is due to the disrupted interaction with SUMO-1.

DISCUSSION

Results shown in this study demonstrate that SAE1/SAE2 and Ubc9 do not discriminate between SUMO-1, -2, and -3. Since SAE1/SAE2 and Ubc9 do not discriminate between the three SUMO paralogues, any surfaces on the three SUMO molecules that are involved in interactions with the E1 and E2 enzymes for conjugation activity should also be conserved. It was shown previously that residues Arg42 and Arg72 in ubiquitin are involved in interactions with E1 (*36, 37*). The analogous residues in SUMO are conserved but not entirely located in the binding surface for SUMO-1 on Ubc9 (Figure 1A). Despite the significant sequence difference between SUMO-1 and -2/-3, their Ubc9 binding surfaces are highly conserved. The binding interfaces of Ubc9 and the three SUMO molecules are highly complementary in their electrostatic potentials and hydrophobicity with the positively charged N-terminal region of Ubc9 interacting with the negatively charged main β-sheet in the ubiquitin domain of SUMO (*25*). The conservation of the E2 binding surface in the three SUMO proteins is not likely to be involved in post-conjugation events because the in vivo functions of the SUMO proteins are likely to be distinct (*19*). The observation that Ubc9 forms thiolester complexes with the three SUMO proteins with almost equal efficiency correlates with the fact
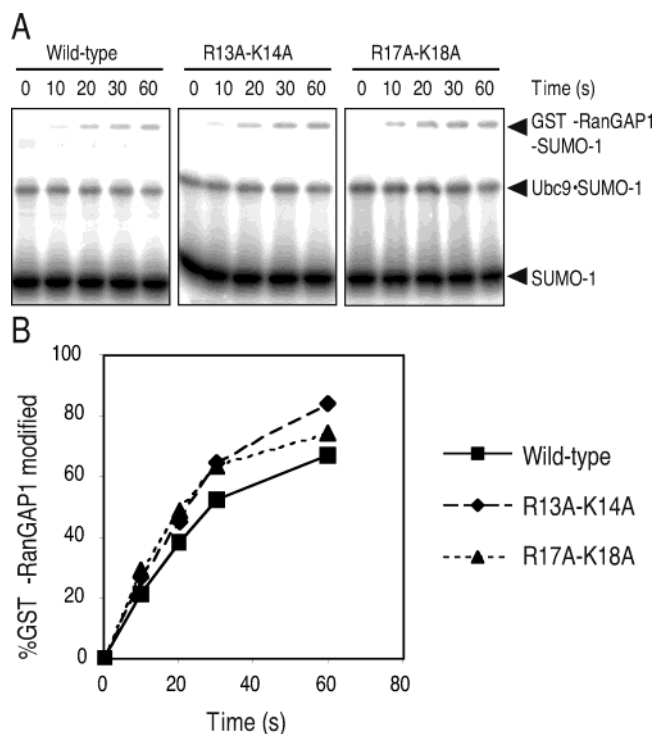
FIGURE 7: N-terminal mutations of Ubc9 do not affect the transfer of SUMO-1 from Ubc9 onto GST-RanGAP1$_{418-587}$. Between 0.3 and 0.5 μM Ubc9·SUMO-1 thiolester complexes were formed for each Ubc9 construct by incubation in the presence of 0.24 mM SAE1/SAE2, 6 μM ^{125}I-SUMO-1, 67 U mL^{-1} IPP, 3.3 mM ATP, and 8.3 mM MgCl$_2$ in 67 mM Tris/HCl pH 7.5 buffer as described in Materials and Methods. Thiolester complex formation was halted by the addition of EDTA, and the transfer reaction was initiated by addition of GST-RanGAP1$_{418-587}$ to 0.2 μM. Ten mL samples were taken 10, 20, 30, and 60 s after substrate addition and terminated by the addition of nonreducing 4 M urea/SDS sample buffer. Reaction products were fractionated by SDS polyacrylamide gel electrophoresis, and radioactive species were detected by phosphorimaging analysis of dried gels. Panel A shows phosphorimage results for wt-Ubc9 (left panel), K13A-R14A-Ubc9 (center panel), and K17A-R18A-Ubc9 (right panel). Free SUMO-1, Ubc9·SUMO-1 thiolester, and RanGAP1$_{418-587}$ are indicated. Quantitation of radioactive species allowed the calculation of the % GST-RanGAP1$_{418-587}$ modified by SUMO-1 for each condition, which is shown graphically in panel B.

that the noncovalent complex between Ubc9 and the three SUMO proteins uses the same surface and binds with nearly identical affinity. This suggests that the conservation of the interactions between Ubc9 and SUMO proteins is important to the conjugation activity. Indeed, residues analogous to the E2 binding surface of SUMO-1 in ubiquitin (L8, I44, and V70) (Figure 1A) have been shown to be important to the conjugation activity of ubiquitin (38).

A recent study of the yeast Ubc9 protein has shown that the E1, Aos1/UBA2, and Smt3p (yeast SUMO) have overlapping binding sites on Ubc9p (32). A recently published structure of APPBP1-UBA3, the heterodimeric E1 enzyme of the ubiquitin-like NEDD8 conjugation pathway, revealed the presence of a Ubl domain in the C-terminus of UBA3 (44), which is likely to be conserved across the E1 protein family. Thus, the Ubl domain of the E1 may interact with E2. Sequence analysis of the equivalent Ubl domain in SAE2 does not reveal any apparent homology with SUMO-1, and in particular, there is no sequence similarity between the β-strands of the predicted Ubl domain of SAE2 and that of SUMO-1, -2, or -3, which are known to form interactions
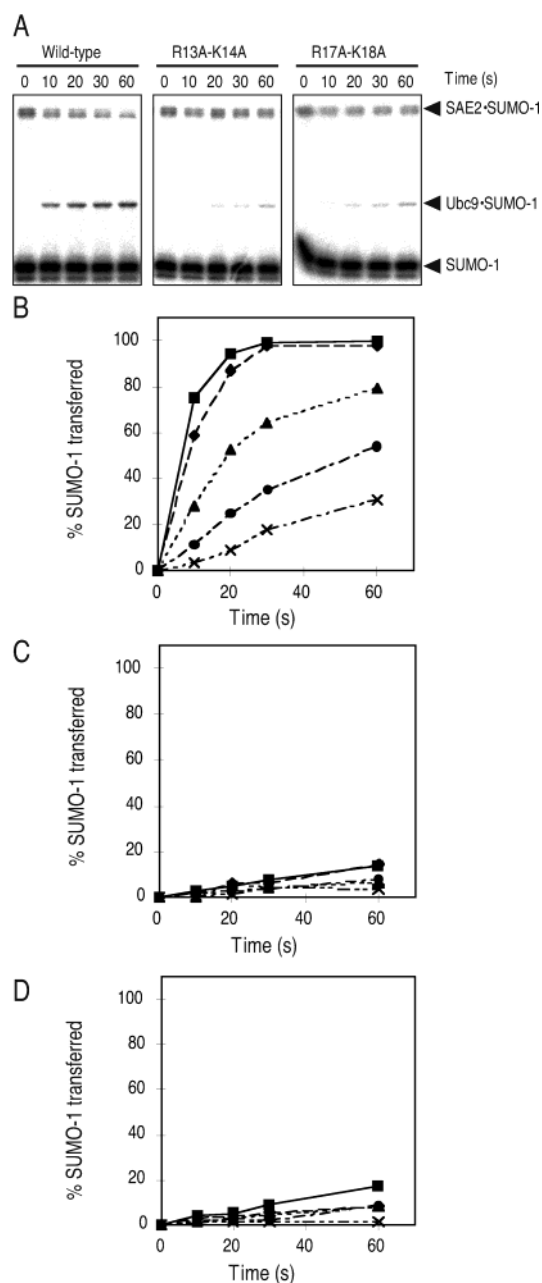

FIGURE 8: N-terminal mutants of Ubc9 affect the SAE1/SAE2 to Ubc9 transesterification step. Reactions were set up such that ~120 nM SAE1/SAE2·SUMO-1 thiolester complexes (prepared as described in Materials and Methods) were mixed with Ubc9 of varying concentrations from 0.2 to 5 μM to initiate a transfer of SUMO-1 from SAE1/SAE2 onto Ubc9. At 10, 20, 30, and 60 s post-initiation, 10 mL samples were taken, and the reactions were terminated by the addition of 4 M urea/SDS sample buffer in the absence of reducing agent. Reaction products were fractionated by SDS–polyacrylamide gel electrophoresis, and radioactive species were detected from dried gels by phosphorimaging. Panel A shows raw phosphorimage data of the transfer reactions for wt-Ubc9 (left panel), R13A/K14A-Ubc9 (center panel), and R17A/K18A-Ubc9 (right panel) at the 5 μM Ubc9 concentration. Bands corresponding to the free ^{125}I-SUMO-1 and the conjugated complexes with Ubc9 and SAE2 are indicated. Quantitative analysis allowed the determination of the absolute quantities of each radioactive species and hence the calculation of the % SUMO-1 transferred from SAE2 or Ubc9. This is represented graphically in panels B–D for wild-type, R13A/K14A, and R17A/K18A-Ubc9 constructs, respectively. Zero time-points were taken prior to transfer initiation. The graph symbols square, rounded diamond, triangle, circle, and cross represent the data corresponding to reactions containing 5, 2, 1, 0.5, and 0.2 μM Ubc9, respectively.

with Ubc9. In addition, the β-sheet of the Ubl domain faces away from the active site Cys residue in the E1 enzyme. However, the β-sheet in SUMO-1 is the binding site for Ubc9. Thus, if this Ubl domain interacts with E2 in a fashion similar to SUMO-1, the active site Cys93 of Ubc9 would face away and be distant from the active Cys residue in E1 and hence would be difficult to be productive for the transfer of SUMO-1 from E1 to E2. However, it is possible that the Ubl domain interacts with Ubc9 in a manner that is distinct from the SUMO-E2 interaction and that both this and the noncovalent interaction between SUMO-1 and Ubc9 are involved in the conjugation pathway.

Both the Ubc9 binding site on SUMO and the SUMO binding site on Ubc9 also function to bind other proteins. The E2 binding surface on SUMO-1 overlaps partially with the binding surface of the deconjugation enzyme Ulp1 (*39*) and partially overlaps with the E1 binding surface of ubiquitin and other Ublps (*36, 37*). The equivalent region to the SUMO binding site on Ubc9 is also used by other E2s and ubiquitin E2 variants (UEV) as a protein interaction site. For example, Mms2, a UEV family member, interacts with the ubiquitin E2 Ubc13 via its N-terminal α-helix (*40, 41*), and the similar region in UbcH7 is involved in interactions with the ubiquitin E3 ligases E6AP and c-Cbl (*42, 43*).

It is intriguing that proteins such as ubiquitin, SUMO, and E2 enzymes use overlapping binding surfaces for the recognition of different proteins. This could be found to be a common theme in protein–protein interactions with our increasing understanding of the molecular details of such interactions. While there may be competition between these binding sites in vitro, it is entirely possible that in vivo occupancy of these sites is strictly controlled by kinetic and spatial mechanisms. The conservation across the ubiquitin and Ublp pathways of the interaction between E2 enzyme and modifier indicates that such binding events are likely to have similar functions and are important features of the conjugation process.

REFERENCES

1. Hershko, A., and Ciechanover, A. (1998) *Annu. Rev. Biochem. 67*, 425−79.
2. Varshavsky, A. (1997) *Trends Biochem. Sci. 22*, 383−7.
3. Hay, R. T. (2001) *Trends Biochem. Sci. 26*, 332−3.
4. Yeh, E. T., Gong, L., and Kamitani, T. (2000) *Gene 248*, 1−14.
5. Muller, S., Hoege, C., Pyrowolakis, G., and Jentsch, S. (2001) *Nat. Rev. Mol. Cell Biol. 2*, 202−10.
6. Lapenta, V., Chiurazzi, P., van der Spek, P., Pizzuti, A., Hanaoka, F., and Brahe, C. (1997) *Genomics 40*, 362−6.
7. Kamitani, T., Kito, K., Nguyen, H. P., Fukuda-Kamitani, T., and Yeh, E. T. (1998) *J. Biol. Chem. 273*, 11349−53.
8. Matunis, M. J., Wu, J., and Blobel, G. (1998) *J. Cell Biol. 140*, 499−509.
9. Mahajan, R., Gerace, L., and Melchior, F. (1998) *J. Cell Biol. 140*, 259−70.
10. Muller, S., Matunis, M. J., and Dejean, A. (1998) *EMBO J. 17*, 61−70.
11. Duprez, E., Saurin, A. J., Desterro, J. M., Lallemand-Breitenbach, V., Howe, K., Boddy, M. N., Solomon, E., de The, H., Hay, R. T., and Freemont, P. S. (1999) *J. Cell Sci. 112*, 381−93.
12. Desterro, J. M., Rodriguez, M. S., and Hay, R. T. (1998) *Mol. Cell 2*, 233−9.
13. Rodriguez, M. S., Desterro, J. M., Lain, S., Midgley, C. A., Lane, D. P., and Hay, R. T. (1999) *EMBO J. 18*, 6455−61.
14. Gostissa, M., Hengstermann, A., Fogal, V., Sandy, P., Schwarz, S. E., Scheffner, M., and Del Sal, G. (1999) *EMBO J. 18*, 6462−71.
15. Goodson, M. L., Hong, Y., Rogers, R., Matunis, M. J., Park-Sarge, O. K., and Sarge, K. D. (2001) *J. Biol. Chem. 276*, 18513−8.
16. Bies, J., Markus, J., and Wolff, L. (2002) *J. Biol. Chem. 277*, 8999−9009.
17. Sachdev, S., Bruhn, L., Sieber, H., Pichler, A., Melchior, F., and Grosschedl, R. (2001) *Genes Dev. 15*, 3088−103.
18. Tatham, M. H., Jaffray, E., Vaughan, O. A., Desterro, J. M., Botting, C., Naismith, J. H., and Hay, R. T. (2001) *J. Biol. Chem. 12*, 12.
19. Saitoh, H., and Hinchey, J. (2000) *J. Biol. Chem. 275*, 6252−8.
20. Rodriguez, M. S., Dargemont, C., and Hay, R. T. (2001) *J. Biol. Chem. 276*, 12654−9.
21. Takahashi, Y., Toh-e, A., and Kikuchi, Y. (2001) *Gene 275*, 223−31.
22. Johnson, E. S., and Gupta, A. A. (2001) *Cell 106*, 735−44.
23. Kahyo, T., Nishida, T., and Yasuda, H. (2001) *Mol. Cell 8*, 713−8.
24. Pichler, A., Gast, A., Seeler, J. S., Dejean, A., and Melchior, F. (2002) *Cell 108*, 109−20.
25. Liu, Q., Jin, C., Liao, X., Shen, Z., Chen, D. J., and Chen, Y. (1999) *J. Biol. Chem. 274*, 16979−87.
26. Miura, T., Klaus, W., Gsell, B., Miyamoto, C., and Senn, H. (1999) *J. Mol. Biol. 290*, 213−28.
27. Nelson, R. M., and Long, G. L. (1989) *Anal. Biochem. 180*, 147−51.
28. Kay, L. E., Keifer, P., and Saarinen, T. (1992) *J. Am. Chem. Soc. 114*, 10663−5.
29. Liu, Q., Shen, B., Chen, D. J., and Chen, Y. (1999) *J. Biomol. NMR 13*, 89−90.
30. Clarke, C., Woods, R. J., Gluska, J., Cooper, A., Nutley, M. A., and Boons, G. J. (2001) *J. Am. Chem. Soc. 123*, 12238−47.
31. Sharrow, S. D., Novotny, M. V., and Stone, M. J. (2003) *Biochemistry 42*, 6302−9.
32. Bencsath, K. P., Podgorski, M. S., Pagala, V. R., Slaughter, C. A., and Schulman, B. A. (2002) *J. Biol. Chem. 277*, 47938−45.
33. Sampson, D. A., Wang, M., and Matunis, M. J. (2001) *J. Biol. Chem. 276*, 21664−9.
34. Lin, D., Tatham, M. H., Yu, B., Kim, S., Hay, R. T., and Chen, Y. (2002) *J. Biol. Chem. 277*, 21740−8.
35. Bernier-Villamor, V., Sampson, D. A., Matunis, M. J., and Lima, C. D. (2002) *Cell 108*, 345−56.
36. Burch, T. J., and Haas, A. L. (1994) *Biochemistry 33*, 7300−8.
37. Whitby, F. G., Xia, G., Pickart, C. M., and Hill, C. P. (1998) *J. Biol. Chem. 273*, 34983−91.
38. Beal, R. E., Toscano-Cantaffa, D., Young, P., Rechsteiner, M., and Pickart, C. M. (1998) *Biochemistry 37*, 2925−34.
39. Mossessova, E., and Lima, C. D. (2000) *Mol. Cell 5*, 865−76.
40. McKenna, S., Spyracopoulos, L., Moraes, T., Pastushok, L., Ptak, C., Xiao, W., and Ellison, M. J. (2001) *J. Biol. Chem. 276*, 40120−6.
41. VanDemark, A. P., Hofmann, R. M., Tsui, C., Pickart, C. M., and Wolberger, C. (2001) *Cell 105*, 711−20.
42. Huang, L., Kinnucan, E., Wang, G., Beaudenon, S., Howley, P. M., Huibregtse, J. M., and Pavletich, N. P. (1999) *Science 286*, 1321−6.
43. Zheng, N., Wang, P., Jeffrey, P. D., and Pavletich, N. P. (2000) *Cell 102*, 533−9.
44. Walden, H., Podgorsk, M. S., and Schulman, B. A. (2003) *Nature 422*, 330−4.